Long term fluctuations of groundwater mine pollution in a sulfide mining district with dry Mediterranean climate: implications for water resources management and remediation

Manuel A. Caraballo[1, 2, 3]·, Francisco Macías[1], José Miguel Nieto[1] and Carlos Ayora[4].

1 Geology Department, University of Huelva, Campus "El Carmen", Av. 3 de Marzo s/n, E-21071 Huelva, Spain

2 Mining Engineering Department, University of Chile, Avda. Tupper 2069, 8370451 Santiago, Chile

3 Advanced Mining Technology Center, University of Chile, Avda. Tupper 2007, 8370451 Santiago, Chile

4 Institute of Environmental Assessment and Water Research, IDÆA – CSIC, Jordi Girona 18, 08034 Barcelona, Spain.

· Corresponding author. Tel.: (+56-2) 29784479

E-mail address: mcaraballo@ing.uchile.cl (Manuel A. Caraballo)

Abstract

Water resources management and restoration strategies, and subsequently ecological and human life quality, are highly influenced by the presence of short and long term cycles affecting the intensity of a targeted pollution. On this respect, a typical acid mine drainage (AMD) groundwater from a sulfide mining district with dry Mediterranean climate (Iberian Pyrite Belt, SW Spain) was studied to unravel the effect of long term weather changes in water flow rate and metal pollutants concentration. Three well differentiated polluting stages were observed and the specific geochemical, mineralogical and hydrological processes involved (pyrite and enclosing rocks dissolution, evaporitic salts precipitation-redisolution and pluviometric long term fluctuations) were discussed. Evidencing the importance of including longer background monitoring stage in AMD management and restoration strategies, the present study strongly advise a minimum 5-years period of AMD continuous monitoring previous to the design of any AMD remediation system in regions with dry Mediterranean climate.

Capsule Abstract

Acid mine drainage management and remediation is shown to be highly dependent of the short- and long-term weather cycles affecting the intensity of this pollution.

Keywords

Acid mine drainage, evaporitic salts, passive treatment systems, climate change

1. Introduction

Acid mine drainage is the term conventionally used to refer the metal pollution and physico-chemical behavior characterizing waters that have been in contact with acidity

39 producing minerals (e.g., sulfides or Fe oxides and hydroxides) in mining districts. These
40 waters exhibit several peculiarities, viz: high metal and sulfate concentration, low pH
41 values and to be commonly buffered by the precipitation of Fe (e.g., schwertmannite) or Al
42 (e.g., hydrobasaluminite) minerals (Bigham and Nordstrom 2000). Moreover, AMD
43 pollution is a worldwide and recalcitrant environmental problem affecting both surface
44 waters and groundwater that typically endures for centuries or even millennia (Younger et
45 al. 2002)).

46 AMD hydrochemistry might be significantly influenced by seasonal fluctuations
47 (Cánovas et al. 2008). Therefore, it is reasonable to expect serious effects of climate change
48 in AMD pollution that are difficult to predict (Nordstrom 2009). The effect of seasonal
49 variations in the pollution of surficial AMD has been widely studied, revealing a clear
50 correlation between drought/wet periods and AMD metal concentration. In this regard, it
51 has been repeatedly documented that the first storm event after a drought period induces a
52 sudden increase in surficial AMD acidity and metal load (Nordstrom 2009, Kimball et al.
53 2007, MacCausland and McTammany 2007, Cánovas et al. 2010). This effect has also been
54 reported as "first flush" and it is attributed to the dissolution of the efflorescent salts that
55 typically cover riverbanks during the dry season. The following storm event of the wet
56 season commonly produces a slight dilution in metal concentration and a pH increase,
57 slightly improving water quality (Cánovas et al. 2010). These seasonal variations can also
58 be recorded as sequences of precipitates within the sediments of AMD affected rivers
59 (Caraballo et al., 2011)

60 The aforementioned "first flush" concept is also applied to groundwater emerging to the
61 surface during the first months following the closure and subsequent flooding of an

62 underground mine (Gzyl and Banks, 2007; Younger, 1997). Most research effort has been
63 placed on the study of AMD groundwater in coal mining districts (Jarvis et al., 2006;
64 Lambert et al., 2004; Younger, 2000; Younger et al., 2002; and papers therein). Whereas
65 only a few studies have looked into groundwater hydrochemical variations in sulfide
66 mining districts (Gray 1998, Nordstrom et al. 2000). In coal districts, the longevity of the
67 "first flush" effect or "vestigial acidity" in the galleries has been estimated to be around 40
68 years, while the persistence of "juvenile acidity" (due to the dissolution of all the remaining
69 pyrite in the galleries) could extent along hundreds of years (Younger, 1997 and 2000). The
70 acidity and metal concentration of the AMD emerging from coal underground mines has
71 been observed to decrease with the time elapsed since the mine closure. This knowledge is
72 essential to design rational planning for the remediation of this devastating pollution.

73 On the other hand, AMD pollution in sulfide mining districts is commonly more severe
74 in terms of metal concentration and most importantly in terms of its longevity (Bigham and
75 Nordstrom 2000). This extreme longevity is due to the enormous amount of pyrite and
76 other sulfides remaining in the galleries of the abandoned mines. In some sulfide mine
77 districts, like the Iberian Pyrite Belt (IPB, SW Spain), the emerging waters from the
78 underground mines correspond to almost 40% of the AMD discharges catalogued in the
79 region (Sánchez-España et al. 2005). A good understanding of both seasonal variations and
80 inter-annual drought and flood events on AMD hydrochemistry is crucial to estimate the
81 intensity and evolution of this pollution and, subsequently to design efficient remediation
82 strategies to accommodate all the system fluctuations over time.

83 The current research analyzes the results obtained after more than 4 years monitoring the
84 emerging waters from the adit of an abandoned underground pyrite mine. The relationship

between the local rainfall regime and weather, the flow rate at the adit and the evolution of AMD metal load is discussed. Galleries at abandoned mines are typically inaccessible, so the geochemical and mineralogical processes occurring within them need to be inferred only by the study of the outflowing AMD. To offer some tools enabling a realistic interpretation of such hidden processes, a set of meteorological, hydrogeochemical and mineralogical parameters were combined using various analytical techniques.

2. Methods and sampling procedure

2.1. Site location

The current study was performed in Mina Esperanza, located in the northern part of the IPB in South-western Spain (37º45´34´´N-6º41´00´´O). The mineralization at Mina Esperanza consists of a massive pyrite deposit with minor amounts of chalcopyrite (Pinedo-Vara, 1963). The enclosing rocks are slates and low grade metamorphic phyllites. The underground works mined a massive pyrite deposit with chalcopyrite, sphalerite and galena (Pinedo-Vara, 1963). The mine was under operation during the first half of the last century. After closure in 1975, the abandoned mine was naturally flooded and, subsequently, polluted water began to flow out of the main adit. As an orphan mine site, there is not any mining company liable for the generated pollution and the mining information available (e.g., underground plans and drawing) is limited or entirely inexistent.

The pluviometric data were provided by the Spanish Weather Service (http://www.aemet.es) and correspond to the automatic station located in El Campillo, 10 km apart from the Mina Esperanza mining area.

107

108 *2.2.* Water sampling and analyses

109 Water samples and flow measurements were taken at least twice a month from March
110 2007 to October 2008, once every 2 month from November 2009 to January 2011 and at
111 least once a month from February 2011 to June 2011. Sampling gap between November
112 2008 and October 2009 was due to logistic problems (impossibility to access the sampling
113 point). The samples were filtered immediately after collection through 0.1 μm Millipore
114 filters on Millipore syringe filter holders, acidified in the field to pH < 1 with Suprapur®
115 HNO_3 and stored at 4 ºC in 60 mL sterile polypropylene containers until analyzed.

116 Temperature and electrical conductivity were measured using a portable CM35 meter
117 (Crison®) with 3 point calibration (147 and 1413 μS/cm and 12.88 mS/cm). The pH and
118 redox potential were measured using a PH25 meter (Crison®) with Crison electrodes.
119 Redox potential and pH were controlled and calibrated using 2 points (240–470 mV) and 3
120 points (pH 4.01–7.00–9.21), respectively, with Crison® standard solutions. Redox potential
121 measurements were corrected to the Standard Hydrogen Electrode to calculate pe.

122 In order to obtain a better understanding of the different processes controlling the
123 outflowing water chemistry, a representative sample from the final period of study was
124 submitted to an evaporation process. The hydrochemistry evolution during the evaporation
125 process and the evaporitic salts generated were analyzed in detail. In addition, the
126 evaporation process was reproduced and studied by means of a geochemical model. A
127 detailed description of the evaporation experiment and modeling is offered in the
128 supplementary information.

129 The concentration of dissolved Fe, Cu, Zn, Na, Al, Ca, Mg, and S in solution was
130 measured by Inductively Coupled Plasma Atomic Emission Spectrometry (ICP-AES) with
131 detection limits of 10 μg/l for Fe, Cu and Zn, 100 μg/l for Na and 50 μg/l for Al, Ca, Mg
132 and S. The concentrations of As, V, Sr, Cd, Pb, Ni and Co were determined by Inductively
133 Coupled Plasma Atomic Mass Spectroscopy (ICP-MS). The detection limits were in the
134 order of 1 μg/l. In the analyses of ICP-AES and ICP-MS, calibration with sets of standards
135 was performed when the regression coefficient exceeded 0.999. Three laboratory standards
136 were analyzed within every 10 samples to check for accuracy. In the analyses of ICP-AES
137 and ICP-MS, dilutions from 1:2 to 1: 100 were performed to ensure that the concentration
138 of the samples was within the concentration range of the standards.

139 Fe(II) and total Fe were determined by colorimetry at 510 nm after complexation in the
140 field by the addition of 0.5% (w/w) 1.10-phenanthrolinium chloride solution to the filtered
141 sample (Rodier et al., 1996), using a DR/890 portable colorimeter (HACH®). The detection
142 limit was 0.3 mg/L and precision was better than 5%; Fe(III) was calculated as the
143 difference between total Fe and Fe(II).

144 X-ray Diffraction (XRD) of randomly oriented powder samples was obtained on a
145 Bruker D5005 X-ray diffractometer with CuKα radiation. The samples were scanned from
146 0 to 60 degrees 2θ with a continuous scan at a rate of 0.025º/18 s.

147 Selected carbon coated samples of precipitates were observed under Scanning Electron
148 Microscopy and Microanalysis (SEM-EDS) to determine the major chemistry, morphology
149 and the sequence of formation of the precipitates from evaporation.

150

151 *2.3.* Statistical multivariate analyses

152 The results of the water chemical analyses and physical-chemical parameters were
153 processed using the programs XLSTAT-Pro v.5.1. Principal Component Analysis (PCA), is
154 a multivariate statistical techniques that allows a large set of data to be simplified and
155 reduced into a smaller number of orthogonal factors (with magnitude and accuracy) to
156 facilitate interpretation by visualizing the correlations that exist between the original
157 variables (Jolliffe, 2002). A PCA was carried out by means of a Spearman's correlation
158 matrix (0.05 significance level, 2 tailed test) to the variables and samples in order to
159 establish possible relations among polluting elements and also to obtain a better
160 understanding of some of the main processes involved in the groundwater pollution and
161 evolution. Due to the high correlation typically showed between dissolved metals and
162 generating processes in AMD environments, only loadings above 0.7 for the new factors
163 generated have been discussed.

164

165 *2.4.* Geochemical modeling

166 Water speciation and mineral saturation indexes were calculated with PHREEQC code,
167 version 2.18.00 (Parkhurst and Appelo, 1999). Thermodynamic data for minerals were
168 obtained from the WATEQ4f database (Ball and Nordstrom, 1991), except for hexahydrite
169 (Delany and Lundeen, 1990), halotrichite (Reardon, 1988), szomolnokite (Tosca et al.,
170 2005) and schwertmannite (Caraballo et al., 2013). The evaporation experiment of the
171 present study was modeled using the Pitzer ion-interaction approach. For more information
172 about the evaporation model the reader is referred to the supplementary information.

173 **3. Results**

3.1. Local climate and adit hydraulic response to the rainfall

The climate in the province of Huelva can be considered as dry Mediterranean type and it is characterized by well-defined dry and wet seasons. Moderate changes can be observed in the climate of the region between hydrological or water years (water years are considered from 1st October of the past year to 30th September of the current year). To illustrate these subtle variations, a decade (2001-2011) of rainfall and temperature records from El Campillo weather station will be summarized. The mean yearly-accumulated rainfall during that decade was around 770 mm with maximum and minimum yearly-accumulated rainfall of 1,223 mm and 401.8 in 2010 and 2005, respectively (Table 1). The mean yearly-temperature (calculated from mean daily-temperatures) oscillated between 16.6 and 17.5 while the maximum and minimum daily values recorded correspond to 43.1 (1st August 2003) and -2.4 (27th January 2005). The calculated standard deviations for each year mean temperature ranged 5.9-7.4, showing that the oscillation between winter and summer mean temperatures is not too drastic (Table 1).

A detailed observation of the trends shown by both rainfall and water discharged from the adit (from March 2007 to August 2011) is offered in figure 1. As can be observed, there is an unequivocal connection between both parameters that is characterized by a poor and steady discharge during the water years with low to moderate rainfalls (2007 and 2008) and by higher discharges and bigger fluctuations during water years affected by important rainfalls (2010 and 2011). The underground network of tunnels and shafts in Mina Esperanza can be understood as a dual porosity aquifer. In accordance to that, a delay between the increase in the accumulated rainfall and its response in the adit discharge can be observed (i.e., December-March 2009-10 and 2010-11, Fig. 1).

197

198 *3.2.* Evolution of the water chemistry

199 Some representative parameters of the adit hydrochemistry for the period 2007-2011 are
200 presented in Figure 2. Within this four-year period, three well-differentiated stages can be
201 observed. A first stage characterized by a steady metal concentration coupled to a constant
202 and low adit outflow (March 2007 to October 2008, Fig. 2). During the final period of this
203 stage, some elements like Fe or As exhibited an increasing tendency whereas the pH values
204 showed a decreasing trend.

205 The second stage covers from November 2009 to July 2010 (Fig. 2). During this time the
206 adit outflow continuously increased, as a response to the intense rainfall received by the
207 region, until reaching a maximum value (4.6 L/s) ten times higher than initial flow rate (0.4
208 L/s, Fig. 2). This gradual and severe outflow rise induced a substantial increase in the metal
209 load of these waters. Within the general increase-decrease cycle shown by the AMD
210 concentration, two different and overlapping behaviors can be differentiated .A common
211 response was observed for some mayor and minor elements like Fe and As (Fig. 2) and
212 other trace metals like V or Ti (Table A1, supplementary information). These elements
213 displayed their maximum values during the sampling on January 2010 (adit discharge = 2.5
214 L/s) and preceding the peak of maximum adit outflow (19^{th} March 2010). On the other
215 hand, some other elements like Al, Cu and Zn (Fig. 2) and also Ca, Cd, Co, Cr, Cu, Mg,
216 Mn, Ni, SO_4 and Sr (Table S1) displayed their maximum concentrations matching the adit
217 maximum discharge. This group of elements can be typified by the behavior of Al and
218 therefore will be referred now on as the Al-group.

219 The third and final stage covers from July 2010 to June 2011 (Fig. 2). This period was
220 characterized by an increase-decrease cycle of the adit outflow. However, this cycle had a
221 negligible effect on the water metal load and hydrochemistry.

222 The Fe(II)/Fe(III) speciation was only measured during the second and third stages. Most
223 of dissolved iron is Fe(II), being the Fe(II)/FeT ratio within 0.92 and 0.98.

224

225 **4. Discussion**

226 *4.1.* AMD hydrochemical response to inter annual climatic fluctuations

227 The Fe/S_{molar} ratio is typically used to infer the extent of the control exerted by pyrite and
228 Fe-sulfates dissolution on AMD hydrochemistry (Cánovas et al., 2010; Sarmiento et al.,
229 2009 and 2011). During the first stage, the adit effluent showed a quite stable metal
230 pollution without marked seasonal variations. The Fe/S ratio increased from 0.3 to the
231 proximity of the theoretical 0.5 value assumed for pure pyrite dissolution (Fig. 3). Ferrous
232 iron oxidation and the subsequent Fe(III) minerals precipitation may account for the
233 observed Fe/S values lower than 0.5. In fact, if these waters are modeled assuming a value
234 of 0.02 for the $Fe(III)/Fe_{total}$ ratio (the lowest value recorded at Mina Esperanza),
235 schwertmannite and jarosite-group minerals are shown to be supersaturated. AMD
236 evaporation and the concomitant precipitation of melanterite can also be responsible for
237 Fe/S values lower than 0.5.

238 The possible effects of seasonal variations in AMD can be targeted using the Zn/Cu_{molar}
239 ratio (Gray 1998, Alpers et al. 1994, Cravotta 1994). The observed correlation between
240 high Zn/Cu_{molar} values and drought periods (or between low Zn/Cu_{molar} values and wet

periods) has been attributed to the preferential Cu uptake (or release) during the precipitation (or dissolution) of melanterite (Alpers et al. 1994). As expected, the specially dry and hot conditions during the summer of 2007 led to an important increase in the Zn/Cu_{molar} values (Fig. 3). On the other hand, a significant decrease in the Zn/Cu_{molar} ratio was recorded coupled to the flow rate increment around May 2008, and followed by a gradual increase of this ratio in the succeeding dry months (Fig. 3).

To untangle the different geochemical and mineralogical processes generating the hydrochemical response of the second stage, it was decided to submit the results to a PCA statistical multivariate analysis. As can be observed in figure 4A, 96.5% of the original variance in the dataset can be represented by 2 factors. The first principal factor (F1) is by far the predominant one and accounts for 81.9% of the variance, while the second one (F2) only explains 14.6%. F1 loading factors are always higher than 0.7 and in many cases even higher than 0.95 (Table A2, supplementary information). The first factor can be assigned to the general increase-decrease cycles observed (Fig. 2 and 4A). Whereas the second factor could be attributed to the well-know control exerted by pH and pe in AMD environments. A detailed inspection of the PCA plot confirmed the existence of two different groups already proposed in the results section (Fig. 4A): pe-group (pe, Fe(II), Fe(III), As, Ti and V) and Al-group (Al, Ca, Cd, Co, Cr, Cu, Mg, Mn, Ni, S, Sr and electrical conductivity). The almost symmetrical positions for pH and pe-group in the PCA plot and the high inverse correlation coefficients observed (pH-pe = -0.80, Table A4, supplementary information) are the typical statistical signs shown by an AMD controlled by pyrite dissolution (Cánovas et al. 2010, Sarmiento et al. 2009). On the other hand, the Al-group is located almost on the same place than the discharge (Q, Fig. 4A) and shows a negligible influence of F2

264 (loadings factors for F2 lower than 0.14, Table A2, supplementary information). This group
265 could be assigned to the dissolution of evaporitic salts in the galleries as a result of the adit
266 flow rate increase.

267 For the sake of clarity, the most plausible sequence of events generating the second stage
268 response will be presented. As already discussed for stage 1, AMD primary source of iron
269 (as ferrous iron) corresponds to the dissolution of pyrite within the galleries (Fig. 4B). As
270 soon as the outflow registered a significant increase in January 2010, both Fe(II) and Fe(III)
271 showed their maximum concentrations (Fig. 4B) due to the combination of an increase in
272 pyrite dissolution (new sources of pyrite are accessible because of the water table rise) and
273 the dissolution of evaporitic salts (mainly melanterite, an extra source of ferrous iron) and
274 schwertmannite/jarosite (source of ferric iron, Fig. 4B). Pursuant to the evaporation
275 experiment performed to the AMD at Mina Esperanza (supplementary information), a
276 sequential precipitation of evaporitic salts beginning with gypsum, $CaSO_4$, followed by
277 melanterite, $FeSO_4$, and finally alunogen, $Al_2(SO_4)_3 \cdot 17H_2O$, is expected. As the adit
278 discharge increase, the underground water reached new regions of the galleries continuing
279 the dissolution of the sequence of evaporitic salts. As a result, the asynchrony between the
280 maximum peaks of pe- and Al- groups was observed (Fig. 2). This sequential evaporitic
281 salts dissolution event is supported by both Fe/S and Zn/Cu molar ratios. As shown in
282 figure 3, as soon as the adit discharge increased (January 2010) the Zn/Cu ratio suffered a
283 pronounced decrease, marking the beginning of the evaporitic salts dissolution. However,
284 the Fe/S ratio showed its maximum drop only after the most intense dissolution of non-iron
285 evaporitic salts (coincident with the Al-group peak) began in March 2010. Once the
286 evaporitic salts were washed out and the adit flow rate began to decrease, Mina Esperanza

AMD progressively resumed its characteristic metal load (Fig. 2) and Fe/S and Zn/Cu ratios (Fig. 3).

The main characteristic defining the third stage is the absence of any significant metal concentration peak despite the existence of an important discharge peak (Fig. 2). However, two synchronous and small decreases in Fe/S and Zn/Cu molar ratios were detected on February 2011 (Fig. 3). This observation suggests the possible redisolution of the evaporitic salts precipitated during the 2 or 3 months of lower flow rate in the transition from stage 2 to stage 3.

4.2. Implications for AMD management and remediation

The hydrochemistry and flow rate of the AMD emerging from the adit of Mina Esperanza can be considered as representative of a high polluted AMD in the IPB (Sánchez-España et al., 2005; Sarmiento et al., 2009). In this regard, the three different stages categorized in the present study could be used as valuable background information to design AMD management and remediation plans. This information is not only relevant for the IPB but also to many other AMD affected mine districts with dry Mediterranean climate around the world, such as in California (Druschel et al., 2004), Western Australia (Biermann et al., 2014), North Africa (Hakkou et al., 2008) and Middle East (Gemici, U., 2008).

Several routine operational parameters (employed in the design of AMD remediation strategies) will be briefly defined to facilitate the discussion in this section. Net acidity (*NA*, g/L as $CaCO_3$ equivalents) was calculated using the following equation after Kirby and Cravotta (2005):

$$NA = 50.045 \cdot (3 \cdot c_{Al} + 2 \cdot c_{Fe} + 2 \cdot c_{Mn} + 2 \cdot c_{Zn} + 10^{-pH}) - alk \quad (1)$$

where c_i is the molar concentration of the ith metal (mol/L), alk is the measured gross alkalinity (mg/L as $CaCO_3$ equivalents) and 50.045 converts moles of charge into grams of $CaCO_3$ equivalents. This parameter can be understood as the AMD potential to generate acidic conditions. Net acidity load (*NAL*, kg/day as $CaCO_3$ equivalents) offers and idea of the "working load" that a remediation system will have to face. In other words, it is an estimation of the net acidity that needs to be neutralized per day. It was generated according the following equation:

$$NAL = NA \cdot Q \quad (2)$$

where *NA* is given in kg/L as $CaCO_3$ equivalents and *Q* is the adit flow rate (L/day). Acidity removal rate (*ARR*) can be expressed according to the surface area (g/m^2/day) or volume (g/m^3/day) of the treatment. This operational parameter is typically used to control the efficiency and size of the remediation system, and can be obtained using the following expressions:

$$ARR = Q \cdot (NA_{in} - NA_{out}) \cdot A^{-1} \quad (3)$$

$$ARR = Q \cdot (NA_{in} - NA_{out}) \cdot V^{-1} \quad (4)$$

where *Q* is the flow rate (m^3/day), NA_{in} and NA_{out} are inflow and outflow net acidity (mg/L as $CaCO_3$ equivalents), and *A* (m^2) and V (m^3) are the treatment surface area and volume, respectively.

The narrow oscillations displayed by net acidity and acidity load values during the first stage (characterized by high metal content and low flow rate) could be considered the most representative state (or steady state) for the AMD at Mina Esperanza (Fig. 5). However, during the second stage (extreme metal content-high flow rate) the outmost pollution was

328 displayed with maximum *NA* (4.05 g/L as $CaCO_3$ equivalents) and *NAL* (1,548 kg/day as
329 $CaCO_3$ equivalents) 1.6 and 11.3 times higher than the average values characterizing stage
330 1 (Fig. 5). On the other hand, the important rainfall during the third stage and the absence
331 of a significant amount of evaporitic salts induced a dilution of the AMD, and subsequently
332 a decrease in the *NA* values comparing with stage 1 (Fig.5). Nevertheless, the *NAL* rose due
333 to the flow rate increment and achieved a maximum value 4.3 times higher than the average
334 values showed during stage 1.

335 Passive treatment systems are the most common choice to remediate AMD at abandoned
336 mining operations (Younger et al., 2002; PIRAMID Consortium, 2003; Watten et al., 2005)
337 This remediation option is typically restricted to flow rates lower than 100 L/s and it is
338 specially indicated for AMD long term remediation (from decades to centuries) due to its
339 economic and environmental sustainability (Johnson and Hallberg, 2005; Ayora et al.,
340 2013). The design of a passive treatment typically follows two consecutive steps: a) set a
341 characteristic pollution to treat, and b) up-scaling the system using a limiting operational
342 parameter. If at all possible, a year of AMD continuous monitoring is commonly advised as
343 a first step to be included in all AMD remediation designs (PIRAMID Consortium, 2003).
344 However, if the results belonging to the first year and a half of the current study were used
345 to design a remediation treatment, it would be clearly insufficient to address the large
346 fluctuations to come during the second and third stages. Therefore, a longer monitoring
347 period, never briefer than 5 years, should be considered a prerequisite for any passive
348 treatment system to be implemented in a dry Mediterranean climate.

349 Consideration should also be given to the influence of the observed AMD long-term
350 fluctuations at the time of up scaling a final passive treatment system. After some decades

of testing and experimentation, the most common passive treatment systems are expected to achieve a distinctive metal removal, showing the following *ARR*: aerobic wetlands from 10 to 30 g/m^2/day (Kruse et al., 2009; Kröpfelová et al., 2009; Szkokan-Emilson et al., 2014), reducing and alkalinity producing systems between 25 and 30 g/m^2/day (PIRAMID Consortium, 2003; Marchand et al., 2010), dispersed alkaline substrate higher than 200 g/m^2/day (Caraballo et al., 2011; Ayora et al., 2013), and oxidizing lagoon from 15 to 100 g/m^2/day (Kruse et al., 2009; Macías et al., 2012). Although it is a common practice to design compartmentalized systems to allow taking a section out of service for maintenance (PIRAMID Consortium, 2003; Younger et al., 2014), passive treatment systems are typically designed to have all their sections working together to achieve the desired *ARR*. If the maximum *NAL* recorded in Mina Esperanza (1,548 kg/day as $CaCO_3$ equivalents) were used to design a passive treatment system, the resulting system would be gigantic (i.e., using dispersed alkaline substrate, the current passive remediation technology with the best *ARR,* the treatment surface area would be as exorbitant as 7,740 m^2) and even worst, it would be underused most of its operation time. A possible solution could be the implementation of a modular system, comprising a main section designed to work under common "working loads" (i.e., stage 1, 700 m^2 dispersed alkaline substrate treating a *NAL* of 140 kg/day as $CaCO_3$ equivalents) and different "emergency" sections designed in parallel to accommodate the *NAL* fluctuations when needed. These emergency sections could be either active or passive depending on the specifics needs and limitations of each field site.

Another important lesson that should be extracted from the study of AMD long-term fluctuations at Mina Esperanza is the need a continuous monitoring in dry Mediterranean

climate. This continuous supervision is essential for the early detection of *NAL* fluctuations and subsequently, to activate the back up treatment sections. By the same token, the traditional use of "pure passive treatment" (infrequent maintenance, low adaptability, limited monitoring and electric energy free) to remediate AMD pollution in dry Mediterranean climate should be discontinued. The next generation of "modular semi-passive" treatment systems should grant a continuous monitoring of the *NAL* to be treated, and a great adaptability to maximize the use of the different modular sections and efficiently address the AMD oscillations.

Last but not least, climate change is directly impacting water resources and hydrogeological/geochemical conditions on Earth and specifically on mining districts. Changes in rainfall patterns, evapotranspiration, and hotter temperature have already been documented in mining districts (Nordstrom, 2009). Mining sites with inadequate design, management, or regulatory oversight will be more vulnerable to impacts of climate change (Anaward, 2013). Therefore, the implementation of adaptive "modular semi-passive" treatments is highly advisable to confront the impacts of climate change on an effective, economic and sustainable way in the current mining sites with dry Mediterranean climate. In this regard, it is highly encouraged to include (if economically possible) the effect of climate change in the design of any future remediation systems. A possible action would be to include a "climate change" safety parameter and increment the calculated maximum operational margins by a factor of two.

5. Conclusions

The present study exposed the significant variations induced in acid mine drainage (AMD) affected groundwater by long-term weather fluctuations. Specifically, three well-differentiated hydrochemical stages were defined after more than 4 years monitoring an AMD in a sulfide mining district with dry Mediterranean climate. The first stage displayed high metal concentration and low flow rate, the second one showed an extreme metal concentration and high flow rate, and finally the third one exhibited a mixed situation between the two previous stages with high flow rate and medium-high metal concentrations. Three different processes were considered as plausible mechanisms responsible of the recorded long-term variability in AMD groundwater. However, the following the three processes were proposed as the most influent ones: 1) pyrite and enclosing rocks dissolution, responsible of the "background" metal concentration; 2) evaporitic salts precipitation-redisolution, accountable for the storage and release of metal pollution in the galleries during the inter-annual dry and wet periods, and 3) pluviometric long term fluctuations, controlling the important variability of the AMD flow rate.

The intense metal load fluctuations presented in the current study have deep implications in the design of AMD remediation strategies. On the light of these results, 5 years of AMD continuous monitoring is strongly advised previous to the design of any AMD remediation system in regions with dry Mediterranean climate. Additionally, these results encourage re-assessing the use of more traditional and inflexible passive treatments to remediate AMD pollution in dry Mediterranean climate should be reassessed. A possible solution could be the implementation of modular systems, comprised by a main section designed to work under common "working loads" coupled to a backup section designed in parallel to accommodate the fluctuations on the acidity load when needed. The next generation of

419 “modular semi-passive” treatment systems should grant a continuous monitoring of the
420 pollution to be treated, and a great adaptability to efficiently address AMD long-term
421 fluctuations.

422

423 **Acknowledgments**

424 This study was financed by the Spanish Ministry of Science an Innovation through the
425 project CGL2013-48460-C2 and project TAAM, FEDER-INNTERCONECTA Program,
426 Ref. ITC-20111083. M.A.C. was financially supported by the Spanish Ministry of
427 Education and the Post-doctoral International Mobility Subprogramme I+D+i 2008–2011.
428 M.A.C. gratefully acknowledge the support form the Advanced Mining Technology Center
429 of the University of Chile.

430

431 **References**

432 Alpers, C.N., Nordstrom, D.K., Thompson, J.M., 1994. Seasonal variations of Zn/Cu ratios
433 in acid-mine water from Iron-Mountain, California. Alpers, C.N. and Blowes, D.W.
434 (eds), pp. 324-344, ACS Symposium Series.

435 Anawar, H. Md, 2013. Impact of climate change on acid mine drainage generation and
436 contaminant transport in water ecosystems of semi-arid and arid mining areas.
437 Physics and Chemistry of the Earth 58–60, 13–21. DOI: 10.1016/j.pce.2013.04.002.

438 Ayora, C., Caraballo, M.A., Macias, F., Rötting, T.S., Carrera, J., and Nieto, J.M., 2013.
439 Acid mine drainage in the Iberian Pyrite Belt: 2. Lessons learned from recent passive

440 remediation experiences. Environmental Science and Pollution research 20, 7837-
441 7853. DOI 10.1007/s11356-013-1479-2.

442 Ball, J.W., Nordstrom, D.K., 1991. User's manual for WATEQ4F with revised
443 thermodynamic database and test cases for calculating speciation of major, trace and
444 redox elements in natural waters. U.S. Geological Survey, water-resources
445 investigation report, 91-183.

446 Biermann, V., Lillicrap, A.M., Magana, C., Price, B., Bell, R.W., Oldham, C.E., 2014.
447 Applicability of passive compost bioreactors for treatment of extremely acidic and
448 saline waters in semi-arid climates. Water Research.
449 DOI:10.1016/j.watres.2014.02.019.

450 Bigham, J.M., Nordstrom, D.K., 2000. Sulfate Minerals: Crystallography, Geochemistry,
451 and Environmental Significance. Alpers, C.N., Jambor, J.L. and Nordstrom, D.K.
452 (eds), pp. 351-403, Reviews in Mineralogy and Geochemistry, Mineralogical Society
453 of America., Chantilly, Virginia.
454 Cánovas, C.R., Hubbard, C.G., Olías, M., Nieto, J.M., Black, S., Coleman, M.L., 2008.
455 Hydrochemical variations and contaminant load in the Río Tinto (Spain) during flood
456 events. Journal of Hydrology 350(1-2), 25-40. DOI:10.1016/j.jhydrol.2007.11.022
457 Cánovas, C.R., Olías, M., Nieto, J.M., Galván, L., 2010. Wash-out processes of evaporitic
458 sulfate salts in the Tinto river: Hydrogeochemical evolution and environmental
459 impact. Applied Geochemistry 25(2), 288-301.
460 DOI:10.1016/j.apgeochem.2009.11.014

461 Caraballo, M.A., Macías, F., Rötting, T.S., Nieto, J.M., Ayora, C., 2011. Long term
462 remediation of highly polluted acid mine drainage: a sustainable approach to restore
463 the environmental quality of the Odiel river basin. Environmental Pollution 159,
464 3613–3619. DOI:10.1016/j.envpol.2011.08.003
465 Caraballo, M.A., Sarmiento, A.M., Sanchez-Rodas, D., Nieto, J.M., Parviainen, A., 2011.
466 Seasonal variations in the formation of Al and Si rich Fe-stromatolites, in the highly
467 polluted acid mine drainage of Agua Agria Creek (Tharsis, SW Spain). Chemical
468 Geology 284, 97-104. DOI:10.1016/j.chemgeo.2011.02.012
469 Caraballo, M.A., Rimstidt, J.D., Macías, F., Nieto, J.M., and Hochella, M.F. Jr. (2013).
470 Metastability, nanocrystallinity and pseudo-solid solution effects on the
471 understanding of schwertmannite solubility. Chemical Geology 360-361, 22-31. e
472 solubility. Chemical Geology 360-361, 22-31.
473 Cravotta, C.A.,1994. Secondary iron-sulfate minerals as sources of sulphate and acidity –
474 geochemical evolution of acidic groundwater at a reclaimed surface coal-mine in
475 Pennsylvania. Alpers, C.N. and Blowes, D.W. (eds), pp. 345-364, ACS Symposium
476 Series.
477 Delany, J., Lundeen, S., 1990. The LLNL thermodynamic database. Tech. Rep. Technical
478 Report UCRL-21658. Lawrence Livermore National Laboratory
479 Druschel, G.K., Baker, B.J., Gihring, T.M., Banfield, J.F., 2004. Acid mine drainage
480 biogeochemistry at Iron Mountain, California. Geochemical Transactions 5 (2), 13.
481 Gemici, U., 2008. Evaluation of the water quality related to the acid mine drainage of an
482 abandoned mercury mine (Alaşehir, Turkey). Environmental Monitoring and
483 Assessment 147, 93–106, DOI: 10.1007/s10661-007-0101-9.

484 Gray, N.F., 1998. Acid mine drainage composition and the implications for its impact on
485 lotic systems. Water Research 32(7), 2122-2134. DOI: 10.1016/S0043-
486 1354(97)00449-1
487 Gzyl, G., Banks, D., 2007. Verification of the "first flush" phenomenon in mine water from
488 coal mines in the Upper Silesian Coal Basin, Poland. Journal of Contaminant
489 Hydrology 92(1-2), 66-86. DOI:10.1016/j.jconhyd.2006.12.001
490 Hakkou, R., Benzaazoua, M., Bussiere, B., 2008. Acid Mine Drainage at the Abandoned
491 Kettara Mine (Morocco): 1. Environmental Characterization. Mine Water and the
492 Environment 27,145–159, DOI 10.1007/s10230-008-0036-6.
493 Jarvis, A.P., Moustafa, M., Orme, P.H.A., Younger, P.L., 2006. Effective remediation of
494 grossly polluted acidic, and metal-rich, spoil heap drainage using a novel, lowcost,
495 permeable reactive barrier in Northumberland, UK. Environmental Pollution 143,
496 261-268.
497 Jolliffe, T., 2002. Principal Component Analysis. Springer Verlag, New York.
498 Johnson, D.B., Hallberg, K.B., 2005. Acid mine drainage remediation options: a review.
499 Science of the Total Environment 338, 3–14. DOI:10.1016/j.scitotenv.2004.09.002
500 Kimball, B.A., Bianchi, F., Walton-Day, K., Runkel, R.L., Nannucci, M., Salvadori, A.,
501 2007. Quantification of changes in metal loadings from storm runoff, Merse river
502 (Tuscany, Italy). Mine Water and the Environment 26, 209-216. DOI:
503 10.1007/s10230-007-0020-6
504 Kirby, C.S., Cravotta, C.A., 2005. Net alkalinity and net acidity 1: theoretical
505 considerations. Applied Geochemistry 20,1920–1940. DOI:
506 10.1016/j.apgeochem.2005.07.002

507 Kröpfelová, L., Vymazal, J., Svehla, J., Stíchová, J., 2009. Removal of trace elements in
508 three horizontal sub-surface flow constructed wetlands in the Czech Republic.
509 Environmental Pollution 157, 1186-1194.
510 Kruse, N.A.S., Gozzard, E., Jarvis, A.P., 2009. Determination of hydraulic residence times
511 in several UK mine water treatment systems and their relationship to iron removal.
512 Mine Water and the Environment 28, 115–123. DOI 10.1007/s10230-009-0068-6
513 Lambert, D.C., McDonough, K.M., Dzombak, D.A., 2004. Long-term changes in quality of
514 discharge water from abandoned underground coal mines in Uniontown Syncline,
515 Fayette County, PA, USA. Water Research 38(2), 277-288. DOI:
516 10.1016/j.watres.2003.09.017
517 MacCausland, A., McTammany, M.E., 2007. The impact of episodic coal mine drainage
518 pollution on benthic macroinvertebrates in streams in the Anthracite region of
519 Pennsylvania. Environmental Pollution 149(2), 216-226. DOI:
520 10.1016/j.envpol.2006.12.030
521 Macías, F., Caraballo, M.A., Nieto, J.M., Rötting, T.S., Ayora, C., 2012. Natural
522 pretreatment and passive remediation of highly polluted acid mine drainage. Journal
523 of Environmental Management 104, 93–100. DOI: 10.1016/j.jenvman.2012.03.027
524 Marchand, L., Mench, M., Jacob, D.L., Otte, M.L., 2010. Metal and metalloid removal in
525 constructed wetlands, with emphasis on the importance of plants and standardized
526 measurements: a review. Environmental Pollution 158, 3447e3461.
527 Nordstrom, D.K., Alpers, C.H., Ptacek, C.J., Blowes, D.W., 2000. Negative pH and
528 extremely acidic mine water from Iron Mountain, California. Environmental Science
529 and Technology 34, 254-258. DOI: 10.1021/es990646v

530 Nordstrom, D.K., 2009. Acid rock drainage and climate change. Journal of Geochemical
531 Exploration 100(2-3), 97-104. DOI: 10.1016/j.gexplo.2008.08.002
532 Parkhurst, D.L., Appelo, C.A.J., 1999. User's Guide to PHREEQC (Version 2) A
533 Computer Program for Speciation, Batch-Reaction, One-Dimensional Transport, and
534 Inverse Geochemical Calculations. USGS Water-Resources Investigations, Denver,
535 Colorado.
536 Pinedo-Vara, I., 1963. Piritas de Huelva. Su historia, minería y aprovechamiento. Summa,
537 Madrid, Spain.
538 PIRAMID Consortium, 2003. Engineering guidelines for the passive remediation of acidic
539 and/or metalliferous mine drainage and similar waste waters. European Commission
540 5th Framework RTD Project no. EVK1-CT-1999-000021 "Passive in situ remediation
541 of acidic mine/industrial drainage" (PIRAMID). University of Newcastle upon Tyne,
542 Newcastle upon Tyne, UK.
543 Reardon, E.J., 1988. Ion interaction parameters for AlSO4 and application to the prediction
544 of metal sulfate solubility in binary salt systems. Journal of Physical Chemistry 92,
545 6426–6431. DOI: 10.1021/j100333a046
546 Sánchez-España, J., López Pamo, E., Santofimia, E., Aduvire, O., Reyes, J., Barettino, D.,
547 2005. Acid mine drainage in the Iberian Pyrite Belt (Odiel river watershed, Huelva,
548 SW Spain): Geochemistry, mineralogy and environmental implications. Applied
549 Geochemistry 20(7), 1320-1356. DOI: 10.1016/j.apgeochem.2005.01.011
550 Sarmiento, A.M., Nieto, J.M., Olías, M., Cánovas, C.R., 2009. Hydrochemical
551 characteristics and seasonal influence on the pollution by acid mine drainage in the
552 Odiel river Basin (SW Spain). Applied Geochemistry 24(4), 697-714. DOI:
553 10.1016/j.apgeochem.2008.12.025

554 Sarmiento, A.M., DelValls, A., Nieto, J.M, Salamanca, M.J., Caraballo, M.A, 2011.
555 Toxicity and potential risk assessment of a river polluted by acid mine drainage in the
556 Iberian Pyrite Belt (SW Spain). Science of the Total Environment 409, 4763-4771.
557 DOI: 10.1016/j.scitotenv.2011.07.043
558 Szkokan-Emilson, E.J., Watmough, S.A., Gunn, J.M., 2014. Wetlands as long-term
559 sources of metals to receiving waters in mining-impacted landscapes. Environmental
560 Pollution 192, 91-103.
561 Tosca, N.J., McLennan, S.M., Clark, B.C., Grotzinger, J.P., Hurowitz, J.A., Knoll, A.H.,
562 Schroder, C., Squyres, S.W., 2005. Geochemical modeling of evaporation processes
563 on Mars: insight from the sedimentary record at Meridiani Planum. Earth and
564 Planetary Science Letters 240, 122–148. DOI: 10.1016/j.epsl.2005.09.042
565 Watten, B.J., Sibrell, P.L., Schwartz, M.F., 2005. Acid neutralization within limestone sand
566 reactors receiving coal mine drainage. Environmental Pollution 137, 295e304.
567 Younger, P.L., 1997. The longevity of mine water pollution: a basis for decision-making.
568 Science of The Total Environment 194-195(0), 457-466. DOI: 10.1016/S0048-
569 9697(96)05383-1
570 Younger, P.L., Banwart, S.A., Hedin, R.S., 2002. Mine Water: Hydrology, Pollution,
571 Remediation., Kluwer Academic Publishers, Dordrecht.
572 Younger, P.L., 2000. Predicting temporal changes in total iron concentrations in
573 groundwater flowing from abandoned deep mines: a first approximation. Journal of
574 Contaminant Hydrology 44(1), 47-69. DOI: 10.1016/S0169-7722(00)00090-5
575 Younger, P.L., Henderson, R., 2014. Synergistic wetland treatment of sewage and mine
576 water: pollutant removal performance of the first full-scale system. Water Research.
577 DOI:10.1016/j.watres.2014.02.024.

578

579 **FIGURE CAPTIONS**

580 Figure 1. Daily-accumulated rainfall (histogram, El Campillo weather station) and adit
581 water flow rate (circles connected by a dotted-line, Mina Esperanza) from March 2007 to
582 August 2011.

583 Figure 2. Time evolution of some pollutants concentration, water pH and flow rate. The
584 dotted areas correspond to the three stages proposed in this study.

585 Figure 3. Fe/S and Zn/Cu molar ratios versus adit AMD outflow during the study period.

586 Figure 4. A) Stage 3 principal component analysis. Alpha significance level 0.05. B)
587 Ferrous, ferric iron and discharge evolution during stages 2 and 3.

588 Figure 5. Adit outflow net acidity (g/L as $CaCO_3$ equivalents) and net acidity load
589 (Kg/day) during the study period.

590

591 **TABLES**

592 Table1. Selected weather parameters in the proximity of Mina Esperanza from 2001 to

593

594 **SUPPLEMENTARY INFORMATION**

595 Appendix 1. AMD evaporation experiment and geochemical model

596 Figure 1A. A) Mineral sequence predicted to form along the evaporation of Mina
597 Esperanza AMD. B) Aggregate of alunogel crystals (Al) sourronding prismatic crystals of
598 melanterite (Me) and gypsum (Gy).

599 Table A1. Summary of water physicochemical parameters and composition for the 61
600 samples comprising this study.

601 Table A2. PCA loadings matrix of the second stage.

602 Table A3. Chemical composition of the water and solids from the evaporation
603 experiment.
604 Table A4. Spearman correlation matrix of the 22 variables analyzed in the waters of the
605 second stage.

Fig. 1

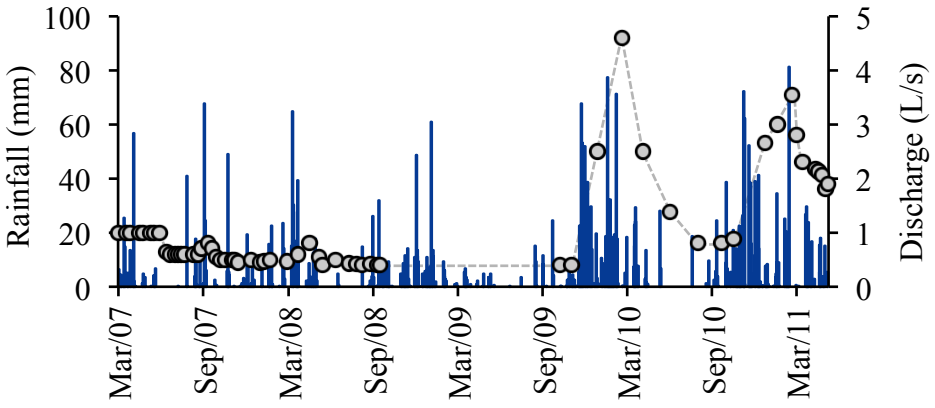

Figure 1. Daily-accumulated rainfall (histogram, El Campillo weather station) and adit water flow rate (circles connected by a dotted-line, Mina Esperanza) from March 2007 to August 2011.

Fig. 2

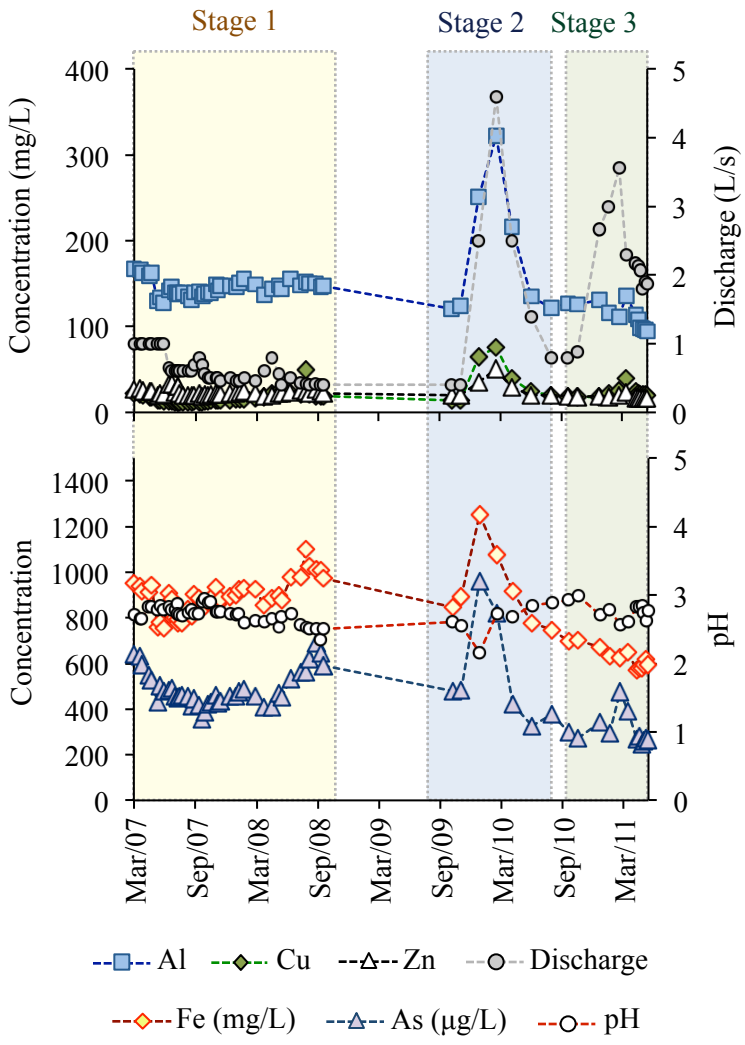

Figure 2. Time evolution of some pollutants concentration, water pH and flow rate. The dotted areas correspond to the three stages proposed in this study.

Fig. 3

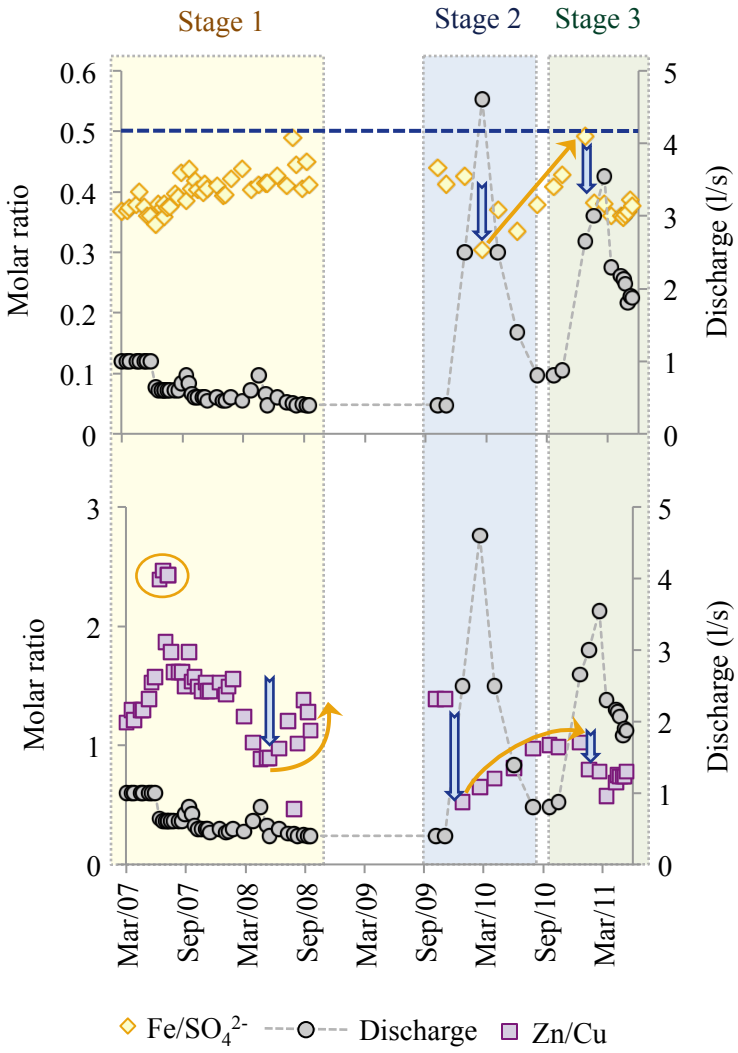

Figure 3. Fe/SO_4^{2-} and Zn/Cu molar ratios versus adit AMD outflow during the study period.

Fig. 4

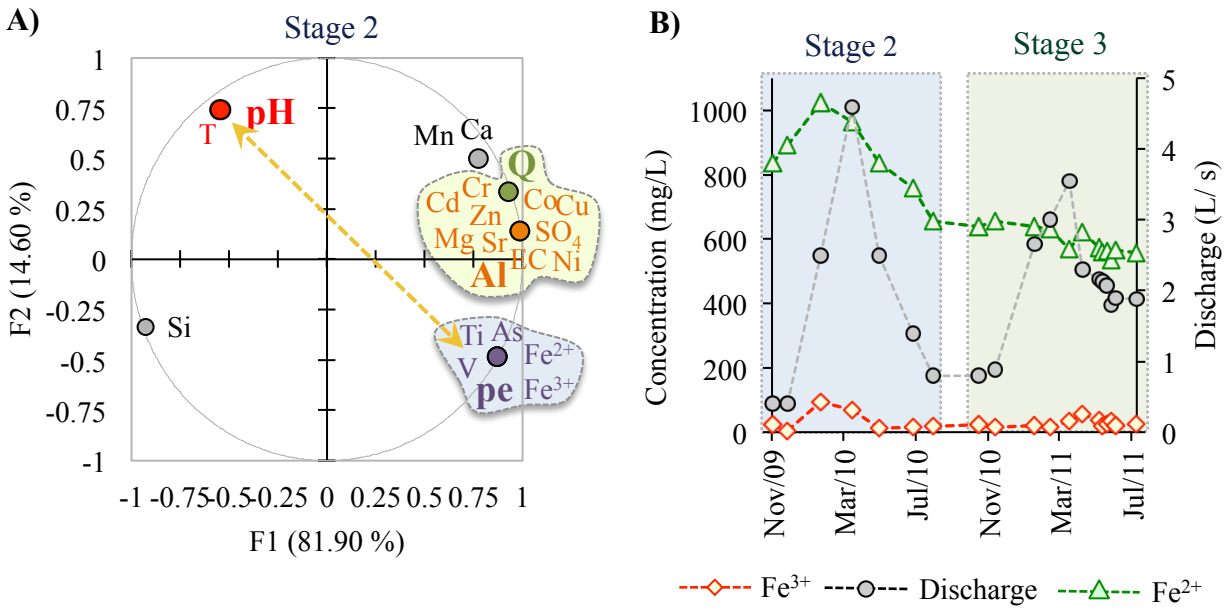

Figure 4. A) Stage 3 principal component analysis. Alpha significance level 0.05. Q = flow rate (L/s), EC = electrical conductivity, pe = redox potential. B) Ferrous, ferric iron and discharge evolution during stages 2 and 3.

Fig. 5

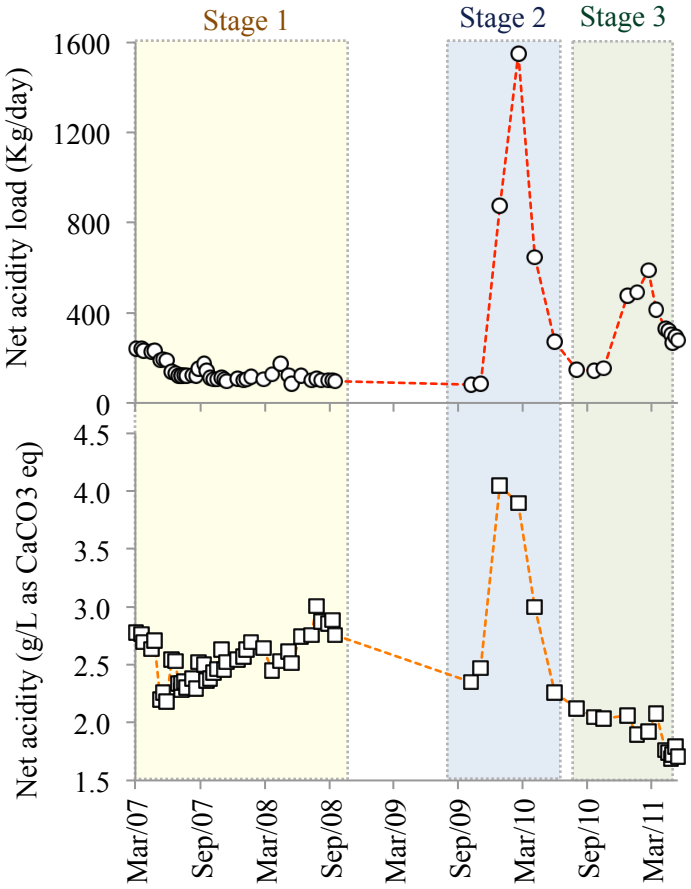

Figure 5. Adit outflow net acidity (g/L as $CaCO_3$ equivalents) and acidity load (Kg/day) during the study period.

Table 1. Selected meteorologic parameters in the proximity of Mina Esperanza for a decade of water years (2001- 2011)

Year	Ac. R. (mm)	T_{mean} (ºC)	$T_{St.\ Dev.}$ (ºC)	$T_{max./min}$ (ºC)
2001	855.4	17.2	6.5	39.3/2.4
2002	750.4	17.0	5.9	38.2/0.0
2003	692.8	17.3	7.0	43.1/0.7
2004	784.4	17.2	7.0	42.3/0.9
2005	401.8	17.1	6.9	41.1/-2.4
2006	699.8	17.2	6.9	40.4/0.0
2007	758.2	16.9	6.1	41.6/-0.2
2008	662.8	16.6	6.3	39.2/0.1
2009	505.4	17.5	7.0	39.3/-1.4
2010	1223	16.7	7.4	40.6/-1.6
2011	1153.6	16.6	6.5	37.5/1.4
2001-11	771.6	17.0	6.7	43.1/-2.4

Ac. R. = Accumulated Rainfall